DOE/NV/25946--277



# ATMOSPHERIC DISPERSION MODEL VALIDATION IN LOW WIND CONDITIONS

*Prepared For*
U.S. Department of Energy,
National Nuclear Security Administration
Nevada Site Office
Las Vegas, Nevada

**FINAL REPORT**

October 1, 2007

Operated by National Security Technologies, LLC, for the U.S. Department of Energy

## DISCLAIMER

This document was prepared as an account of work sponsored by an agency of the U.S. Government. Neither the U.S. Government nor any agency thereof, nor any of their employees, makes any warranty, express or implied, or assumes any legal liability or responsibility for the accuracy, completeness, or usefulness of any information, apparatus, product, or process disclosed, or represents that its use would not infringe upon privately owned rights. Reference herein to any specific commercial product, process, or service by trade name, trademark, manufacturer, or otherwise, does not necessarily constitute or imply its endorsement, recommendation, or favoring by the U.S. Government or any agency thereof. The views and opinions of authors expressed herein do not necessarily state or reflect those of the U.S. Government or any agency thereof.

Contact: Patrick Sawyer
Nonproliferation Test and Evaluation Complex
Operations Manager
702-295-4466
sawyerps@nv.doe.gov

ABSTRACT

**Atmospheric Dispersion Model Validation for Low Wind Speed Conditions**

By

Patrick Shawn Sawyer

Atmospheric plume dispersion models are used for a variety of purposes including emergency planning and response to hazardous material releases, determining force protection actions in the event of a Weapons of Mass Destruction (WMD) attack and for locating sources of pollution. This study provides a review of previous studies that examine the accuracy of atmospheric plume dispersion models for chemical releases. It considers the principles used to derive air dispersion plume models and looks at three specific models currently in use: Aerial Location of Hazardous Atmospheres (ALOHA), Emergency Prediction Information Code (EPIcode) and Second Order Closure Integrated Puff (SCIPUFF). Results from this study indicate over-prediction bias by the EPIcode and SCIPUFF models and under-prediction bias by the ALOHA model. The experiment parameters were for near field dispersion (less than 100 meters) in low wind speed conditions (less than 2 meters per second).

TABLE OF CONTENTS

LIST OF TABLES

LIST OF FIGURES

## LIST OF ABBREVIATIONS

| | |
|---|---|
| ALOHA | Aerial Location of Hazardous Atmospheres (EPA dispersion model) |
| Avg | average |
| $C_o$ | observed concentration (ppm or $mg/m^3$) |
| $C_p$ | predicted concentration (ppm or $mg/m^3$) |
| $^oC$ | degrees Celsius |
| cm | centimeter(s) |
| cm/s | centimeters per second |
| DOD | U.S. Department of Defense |
| DOE | U.S. Department of Energy |
| EPA | U.S. Environmental Protection Agency |
| EPIcode | Emergency Prediction Information Code (DOE model) |
| eV | electronvolt |
| FAC2 | fraction of observations within a factor of 2 of prediction |
| FB | fractional bias |
| H | effective release height above ground (measured in meters) |
| HPAC | Hazard Prediction Assessment Capability (DoD Tool Kit) |
| IP | ionization potential |
| kg/h | kilograms per hour |
| L | The Monin-Obukhov length (L) is the height above ground where the Richardson Number is unity. |
| m | meter(s) |
| m/s | meters per second |
| MG | geometric mean bias |
| min | minute(s) |
| NMSE | normalized mean square error |
| NPTEC | Nonproliferation Test and Evaluation Complex |
| NSTec | National Security Technologies, LLC |
| NTS | Nevada Test Site |
| ppb | parts per billion |
| ppm | parts per million |
| Q | release rate (measured in kilograms per hour) |
| R | correlation coefficient |
| s | second(s) |
| $s/m^3$ | seconds per meter cubed |
| SCIPUFF | Second Order Closure Integrated Puff (Titan Corporation model) |
| SDRD | Site Directed Research and Development |
| u | average wind speed (measured in meters per second) |
| uv | ultraviolet |
| VG | geometric variance |

| | |
|---|---|
| $x$ | downwind distance from the source (measured in meters) |
| $y$ | crosswind distance from the source (measured in meters) |
| $z$ | vertical distance above ground (measured in meters) |
| $z_o$ | Surface Roughness Length (measured in meters) |
| $\sigma_\theta$ | standard deviation in wind direction |
| $\sigma_y$ | horizontal dispersion coefficient (measured in meters) |
| $\sigma_z$ | horizontal dispersion coefficient (measured in meters) |

ACKNOWLEDGEMENTS

I wish to thank my advisory committee, Dr. Vernon Hodge, Dr. Balakrishnan Naduvalath, Dr. Mark Green and Dr. Pradip Bhowmik for their insights and advice which guided me through this endeavor. I would also like to thank my research partners, Dr. Kevin Kyle and Dr. Richard Venedam for their contributions to the experiment. I wish to thank Mr. William Steorts, USAF, for granting me permission to use the US Air Force AFTAC version of SCIPUFF and Dr. Ian Sykes, developer of the SCIPUFF code for his assistance with model inputs.

This effort could not have been achieved without the hard work and dedication of my team at the Nonproliferation Test and Evaluation Complex, Shawn Line, Bill Huth, Ross Lanko, Lyle Warren and Lyle McKenzie. This research was funded through the US Department of Energy's Site Directed Research and Development program, administered by the Nevada Test Site operations contractor, National Security Technologies, LLC.

I also wish to acknowledge my Environmental Studies Professors, Dr. David Hassenzahl and Dr. Timothy Farnham, who provided me with the inspiration to complete my graduate studies at UNLV and Dr. Krystyna Stave, my Graduate Coordinator, who guided me through the processes required to reach graduation.

# CHAPTER 1

# INTRODUCTION

## Purpose of the Study

Gaussian plume dispersion models are widely used by emergency response personnel as well as environmental regulators. In wind speeds greater than 2 meters per second (m/s), advection dominates and the plume forms a cone shape with the tip at the plume source. Within this cone, chemical species generally disburse in a Gaussian pattern, allowing for generally accurate prediction of downwind chemical plume concentrations by the plume models. In low wind conditions (0 to 2 m/s), advection no longer dominates over diffusion, and the Gaussian distribution may no longer be valid. This may result in over-prediction of plume centerline concentrations under weak wind conditions.

In this qualitative research experiment, several plumes were produced in low wind conditions, and plume concentration data were collected to compare against three publicly available dispersion models. The models chosen for evaluation are Aerial Location of Hazardous Atmospheres (ALOHA), Emergency Prediction Information Code (EPIcode), and Second Order Closure Integrated Puff (SCIPUFF). ALOHA and EPIcode are used by federal agencies for emergency planning and response operations and SCIPUFF is the atmospheric dispersion model used by the Defense Department as part of their Hazard Prediction Assessment Capability (HPAC), program. The goal of this

research is to determine the accuracy of these commercial models in predicting plume concentration in low wind conditions. This research addresses the following question: How accurate are Gaussian atmospheric dispersion models at predicting plume concentrations in low wind conditions?

## Research Questions

### Null Hypothesis

H0:Gaussian chemical plume dispersion models underestimate plume concentrations in weak wind conditions.

### Alternative Hypothesis

H1:Gaussian chemical plume dispersion models overestimate plume concentrations in weak wind conditions.

H2:Gaussian chemical plume dispersion models accurately predict plume concentrations in weak wind conditions.

## Significance of the Study

Plume dispersion models are used to determine down range chemical concentrations and hazard zones. The model predictions are used to assist decision makers in determining what protective actions, if any, need to be taken to ensure protection of personnel and the environment. Model prediction accuracy is therefore an important

public safety issue. Unfortunately, there are few studies that demonstrate the accuracy of predictions in low wind speed conditions. Those studies that do exist usually involve the use of tracer gasses such as sulfur hexafluoride or carbon dioxide, which act as dense gasses and may behave differently from common industrial gasses such as ammonia. The existing studies are also primarily long-range experiments with receptor locations hundreds to thousands of meters (m) down range.

This study provides plume dispersion data from a set of point sensors arranged in four circular rings at distances of 10, 25, 50, and 100 m from the release source. The rings are necessary due to the significant variability in wind direction under low wind speed conditions. Wind direction can vary over $100^{o}$ in a short period of time when wind speeds are below 2 m/s (Venkatram et al., 2004).

Ammonia, ethylene, and propylene are used to provide a range of molecular weights representing lighter than air gasses, neutrally buoyant gasses, and heavier than air gasses respectively. The study looks at near field dispersion (up to 100 m down range). This is where the highest concentrations would be found and where the greatest uncertainty in plume dispersion exists.

# CHAPTER 2

# REVIEW OF RELATED LITERATURE

## Atmospheric Dispersion Model History and Theory

Atmospheric dispersion models play an important role in protecting public health and safety.These models are used to predict downwind chemical concentrations using mathematical formulas for atmospheric diffusion. They are used by emergency response personnel and the military to determine protective action distances. They are also used by governmental regulatory agencies to assist in zoning of industrial facilities and determining the source of hazardous pollutants. Because of the importance of these models, it is critical that the information derived be compared against real data to provide confidence that the model predictions are accurate. Models that underestimate plume concentrations pose a threat to human health and the environment, while models that overestimate plume concentrations may have serious economic consequences (Chang and Hanna, 2004).

Atmospheric plume dispersion modeling dates back to the 1920s. Following World War I, scientists tried to estimate chemical plume concentrations from poison gas attacks under various wind conditions (Macdonald, 2003). The British conducted the Porton

smoke experiments, which provided data on plume spread as a function of distance (Peterson et al., 1999). In the decades since, scientific understanding of atmospheric physics and chemistry have refined these models to the point where they are used by regulatory agencies and are codified in the Title 40 U.S. Code of Federal Regulations Part 51.

Modern atmospheric dispersion models are computer programs that predict downwind plume concentrations based on input variables including source strength, plume temperature, stack height, stack diameter, terrain features such as surface roughness, and meteorological conditions such as wind speed, atmospheric stability, and the presence of an inversion layer. The models use various mathematical formulas that describe complex phenomena such as diffusion to calculate downwind species concentrations (Macdonald, 2003).

There are two ways of describing atmospheric dispersion. The Eulerian method examines the behavior of a species relative to a fixed coordinate system in which the concentration is determined by taking a material balance over a volume element. The Lagrangian method considers the concentration changes relative to the moving fluid. Unfortunately, neither method will produce an exact solution for the mean concentration of a species in a fluid, necessitating the use of simplifying assumptions (Seinfeld and Pandis, 1998).

Chemical species released into the atmosphere are carried away by the prevailing air mass through advection. The species are dispersed by turbulent eddies. In moderate and strong wind speeds, the advection term dominates over diffusion, and the resulting plume forms a cone shape with the apex being the point source. Inside the cone, the plume

disburses in a Gaussian pattern (i.e., a vertical and horizontal bell shaped curve). In low wind speeds (less than 2 meters per second), the plume is no longer uniformly cone shaped as diffusion in the horizontal and vertical directions becomes more important than advection in the general wind direction (Sharan et al., 1995). The Gaussian diffusion equation assumes wind speed and eddy diffusivities are constant with height (Lin and Hildemann, 1996).

Low wind speeds are associated with a phenomenon called meander, which is a horizontal oscillation of the local atmosphere. As wind velocity decreases below a certain threshold, it is no longer possible to define a mean wind direction. These oscillations are independent of atmospheric stability or topography and are related to the equilibrium between the coriolis force and the pressure gradient (Oettl et al., 2005).

Hanna et al. (1982) give the basic form of the Gaussian plume model as:

$$\chi(x,y,z) = \frac{Q}{2\pi\sigma_y\sigma_z u} \exp\left[-\frac{1}{2}\left(\frac{y}{\sigma_y}\right)^2\right] \left\{ \exp\left[-\frac{1}{2}\left(\frac{z-H}{\sigma_z}\right)^2\right] + \exp\left[-\frac{1}{2}\left(\frac{z+H}{\sigma_z}\right)^2\right] \right\}$$

Where:

$\chi$ = atmospheric concentration ($mg/m^3$)

Q = release rate (mg/s)

x = downwind distance from the source (m)

y = crosswind distance from the source (m)

z = vertical distance above ground (m)

H = effective release height above ground (m)

$\sigma_y$ = horizontal dispersion coefficient, as a function of y representing the standard deviation of the concentration distribution in the crosswind axis direction (m)

$\sigma_z$ = vertical dispersion coefficient, as a function of z representing the standard deviation of the concentration distribution in the vertical axis direction (m)

u = average wind speed (m/s)

To account for reflection of the plume at the surface, the last term in the equation represents a mirror source located H m beneath the surface (Thoman et al., 2005).

Dispersion coefficients, $\sigma_y$ and $\sigma_z$, can be determined by calculating the standard deviations of the prevailing wind angles or by using a standard reference curve based on atmospheric stability class (Thoman et al., 2005). Reference curves were developed by Pasquill and later modified by Gifford. In general, higher levels of atmospheric instability will result in greater atmospheric dispersion and lower peak plume concentrations. Atmospheric stability has been divided into six classes ranging from A, for very unstable conditions, to F for very stable conditions. Since local terrain also affects atmospheric dispersion, different sets of dispersion curves have been developed for urban and rural settings. Urban areas generate significantly more mechanical turbulence than flat rural settings due to increased surface roughness (Thoman et al., 2005).

Hanna and Chang (1992) point out that the use of Pasquill-Gifford curves for many simple dispersion models fix the dispersion coefficients, $\sigma_y$ and $\sigma_z$, representing an over-simplification of the boundary layer variables. Real-time observation of all the boundary layer parameters is rarely achievable, requiring the use of parameters that are frequently available, such as percent cloud cover and 10 m wind speed. The parameterization works

well for ideal conditions, (wind speeds greater than 5 m/s and strong net solar radiation – Q > 100 Watts per square meter), but are not valid for non-ideal conditions (light winds and weak solar radiation). Non-ideal conditions can produce relative errors in excess of 100 percent (Hanna and Chang, 1992).

Since wind speed is dependent on elevation, most models require the elevation that the wind speed is measured at be included in the model input. Wind speed at the release point is usually used for elevated sources, and a 10 m wind speed is used for ground level releases (Macdonald, 2003). The models apply a correction factor to the wind to represent the wind speed at the reference height used to calculate the dispersion. The correction factors are a function of the atmospheric stability class. For the EPIcode model the reference height 2 m, and for the ALOHA model the reference height is 3 m (Thoman et al., 2005). Wind speed normally increases with height, causing the upper portion of the plume to pull away from the portion of the plume near the ground. The Gaussian plume dispersion equation assumes a constant wind speed, ignoring the shear effect the higher wind speed at height has on the plume (Wang, 1996).

Evaluation of model predictions in low wind conditions is important due to the fact that these conditions can be expected to frequently occur, especially at night when there is a lack of solar energy driving atmospheric circulation. These low wind speed stable conditions will result in peak plume concentrations due to the lack of atmospheric dispersion. Gaussian models may produce an overestimation of plume concentration in low wind conditions if they do not account for along-wind diffusion. Pasquill stability classes were specifically designed to be applied in wind speeds greater than 2 m/s (Sharan et al., 1995). As mentioned earlier, during low wind speed conditions, wind

direction can vary significantly in a short period of time. This variability in wind direction, ($\sigma_\theta$), can be as large as $100^o$ (Venkatram et al., 2004).

Another factor to account for is the buoyancy of the plume. The vapor density of the chemical species being released can have a significant impact on how the plume behaves in the environment. In general, lighter than air species will raise while heavier than air species will sink. Heavier than air gas, also known as dense gas, undergoes gravitational slumping characterized by increased horizontal spreading and reduced vertical spread as compared to a neutrally buoyant plume (Thoman et al., 2005). Commercial models such as ALOHA include a dense gas algorithm to correct for heavier than air species. The difference in resulting plume concentrations between the Gaussian plume predictions and the dense gas model predictions can vary significantly (Thoman et al., 2005).

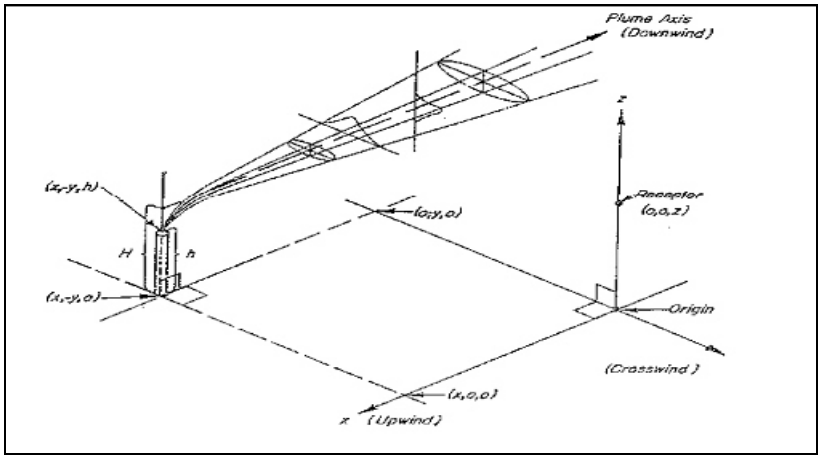


*(U.S. Environmental Protection Agency [EPA], 2004)*

*Figure 1 Gaussian Plume Dispersion*

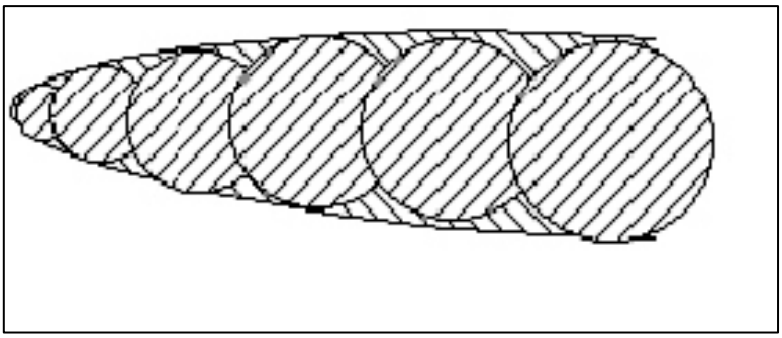

*(EPA, 2004)*

*Figure 2 Gaussian Puff Dispersion*

## Dispersion Model Validation

Since basic Gaussian plume models make simplifying assumptions regarding dispersion, most modern dispersion modeling programs apply various algorithms to account for such factors as atmospheric stability, inversion layers, buoyancy induced dispersion, ground deposition, and terrain features (Macdonald, 2003). Field trials are used to validate the model results.

Chang and Hanna (2004) propose that atmospheric dispersion models can be validated scientifically, statistically, or operationally. The scientific approach examines the mathematical formulas and their underlying assumptions of physics and chemistry to determine their accuracy. Statistical analysis involves a direct comparison of model predictions versus actual observations. An operational evaluation looks at the models ease of use, the user model interface, output format, and features such as error checking (Chang and Hanna, 2004).

Model validation can be problematic due to the random nature of the physical processes that produce uncertainty in the model predictions. Models can only be evaluated by demonstration of the agreement between the model and several sets of

observations (Oreskes et al., 1994). The difficulty with model evaluations arises from the fact that uncertainty in the model predictions may be due to input data errors or errors in the model code, while uncertainty in observations may be due to measurement errors or random atmospheric motions (Chang and Hanna, 2004).

Chang and Hanna (2004) propose model evaluation of such factors as concentration over a sampling line, plume width along a sampling line, maximum dosage along a sampling line, and plume arrival and departure times among other potential model outputs. Data should be analyzed in various ways prior to performing a statistical analysis of the model performance to determine any unknown relationships that might exist (Chang and Hanna, 2004). Quantile-quantile and scatter plot analyses can uncover biases at high or low concentrations or the magnitude of a model's under-prediction or over-prediction (Chang and Hanna, 2004).

Standard criteria for statistical evaluation of model performance include fractional bias (FB), geometric mean bias (MG), normalized mean square error (NMSE), geometric variance (VG), correlation coefficient (R), and fraction within a factor of two (FAC2). These criteria are defined as follows:

$$FB = \frac{(\overline{C}_o - \overline{C}_p)}{0.5(\overline{C}_o + \overline{C}_p)} \qquad MG = \exp(\overline{\ln C_o} - \overline{\ln C_p})$$

$$NMSE = \frac{\overline{(C_o - C_p)^2}}{\overline{C}_o \overline{C}_p} \qquad VG = \exp[\overline{(\ln C_o - \ln C_p)^2}]$$

$$R = \frac{\overline{(C_o - \overline{C}_o)(C_p - \overline{C}_p)}}{\sigma_o \sigma_p}$$

FAC2 = fraction of data for which $0.5 \leq (C_p/C_o) \leq 2$

The subscripts o and p refer to observed and predicted values (Yadav and Sharan, 1996).

FB is an indication of the over-prediction or under-prediction of a particular model. Values can range from -2 to 2 with zero being ideal. The NMSE is a measure of the deviation between the predicted and observed data. A smaller NMSE indicates a more accurate model prediction. R measures the degree of agreement between the variables with an ideal value being unity. FAC2 is a ratio of the model predictions that are within a factor of two of the observed data with a value of unity being ideal (Yadav and Sharan, 1996). MG and the VG are logarithmic measures and are thus particularly useful for analyzing very high or very low values. Model predictions that match observation would show an MG and VG of 1.0 (Chang and Hanna, 2004).

## Previous Experiments

Several dispersion experiments have been conducted to provide observational data for model evaluation. Between 1985 and 1987, the U.S. Department of Energy (DOE) sponsored the Desert Tortoise and Goldfish experiments on Frenchman Flat at the Nevada Test Site (NTS). These experiments looked at the dispersion characteristics of a cryogenic release of ammonia and hydrogen fluoride. An interesting observation to emerge from these experiments is a variation in the appropriate value to use for surface roughness length, $z_o$. The Desert Tortoise observations suggest a $z_o$ of 0.003 m while the Goldfish data suggests a $z_o$ of 0.0002 m (Hanna et al., 1993). In 1995, the DOE sponsored the Kit Fox experiment, also on Frenchman Flat. This experiment consisted of 52 releases of carbon dioxide over a model field simulating a typical refinery. The purpose of the experiment was to determine the ability of the HEGADAS 3+ dense gas

dispersion model to account for increased surface roughness. Roughly 90% of the observations were within a factor of 2 of the model predictions (Hanna and Chang, 2001).

In 1995 and 1996, sulfur hexafluoride was released near Galen, Montana, from a continuous (20 [min]) source located 2 m above the ground. Wind data were collected from a height of 3.5 m. Most of the releases took place in unstable atmospheric conditions. The data were used to evaluate empirical and theoretical techniques for estimating diffusion coefficients (Peterson et al., 1999).

In October 2000, DOE conducted the Urban 2000 experiment involving the release of sulfur hexafluoride in downtown Salt Lake City. The releases were 1 hour in duration and took place at ground level. The purpose of the experiment was to determine the effect of a terrorist release of a chemical or biological agent in an urban environment. This experiment, along with a similar urban experiment in San Diego in 2002, demonstrated good general agreement with model predictions for urban dispersion (Hanna et al., 2003). These experiments led to the development of formulas for estimating atmospheric variables such, as turbulence and dispersion, in urban areas. Hanna et al. (2003) note that in low wind conditions, with large $\sigma_\theta$, upwind dispersion is possible. An interesting observation of the Salt Lake City data suggests that in wind speeds less than 1.5 m/s and downwind distances in excess of 100 m, the maximum concentration is independent of wind speed (Hanna et al., 2003).

## Atmospheric Dispersion Model Descriptions

### ALOHA

ALOHA is an acronym for Aerial Locations of Hazardous Atmospheres. It is available for download, free of charge, from http://www.epa.gov/ceppo/cameo/aloha.htm. It is capable of modeling both neutrally buoyant and dense gas releases. ALOHA uses Gaussian and heavy gas dispersion algorithms to predict downwind concentrations from a variety of sources including evaporating pools, pressurized releases from pipes, and continuous sources such as stacks. ALOHA does not model reactive chemicals or particulates. It also does not account for the positive buoyancy from a heated gas source. ALOHA uses the A through F stability classes and has the ability to determine which class to use based on modeler inputs of cloud cover, wind speed, and time of day. ALOHA version 5.4.1 was downloaded from the EPA website in February 2007 for use in this experiment. This model summary is from the Office of the Federal Coordinator for Meteorology web site at http://www.ofcm.noaa.gov/atd_dir/pdf/aloha.pdf.

### EPIcode

EPIcode is an acronym for the Emergency Prediction Information code. This model is used at Lawrence Livermore National Laboratory for emergency response and planning. It is available from Homann Associates, Inc., at http://www.epicode.com. EPIcode can model gas, vapor, and aerosol releases. Its Gaussian dispersion puff and plume algorithms predict downwind concentrations for buoyant and neutrally buoyant chemical species. EPIcode has an internal chemical library of over 2,000 substances. This experiment used EPIcode version 7.0 with the 2007 library.

## SCIPUFF

SCIPUFF is an acronym for Second order Closure Integrated Puff. This model is part of the DoD's Hazard Assessment System for Consequence Analysis (HASCAL), which in turn provides the plume prediction capability of the HPAC program. The SCIPUFF program was developed by Titan Corporation and is available for download from http://www.titan.com/products-services/336/download_scipuff.html. SCIPUFF is a Lagrangian puff dispersion model that is based on a second order closure theory to predict dispersion rates from a series of Gaussian puffs that represent a time dependent concentration field. The version of SCIPUFF used for this experiment (Breeze SCIPUFF AFTAC version 1.3.6) was purchased from Breeze Software. It includes a graphical user interface and displays results in tabular format for easier analysis. This model summary is from the Office of the Federal Coordinator for Meteorology web site, http://www.ofcm.noaa.gov/atd_dir/pdf/scipuff.pdf.

## Summary

Dispersion of a chemical species in the atmosphere is primarily dependent on turbulence in the atmospheric boundary layer. Since turbulence is random and cannot be predicted, mathematical formulas for standard deviation and variance are employed to estimate the effect of turbulence. These estimations contain inherent errors due to the variability of natural phenomenon. This natural variability rules out the possibility that any model will predict observed data 100% of the time (Chang and Hanna, 2004).

Examination of model performance in low wind conditions is important due to the frequency of such conditions and the high potential hazard associated with toxic

emissions in such conditions (Sharan et al., 2002). Moreira et al. (2005) point out that Gaussian models do not perform well in low wind speed conditions since down wind diffusion is neglected. Standard Gaussian dispersion models tend to over-predict peak concentration and under-predict plume spread in low wind conditions (Yadav and Sharan, 1996). Cirillo and Poli (1992) demonstrate that the standard Gaussian models can be significantly enhanced by consideration of diffusion along the mean wind direction.

Models play an important role in providing general information about the consequences of a chemical release. As long as the model has been evaluated against real data, and as long as the assumptions made by the model are known, then model predictions are useful pieces of information that can be used to make sound decisions on health and safety or public policy. Confidence in model predictions is enhanced by comparison with observed data. Low wind conditions present models with a significant challenge since most models use Pasquill-Gifford stability curves that are only valid in winds above 2 m/s. Research to evaluate model predictions in low wind speed conditions will provide model users with an understanding of the limitations of these models.

Research to collect low wind speed atmospheric plume dispersion data will be useful in the development of improved algorithms for predicting the effects of turbulent dispersion on downwind chemical concentration. This research focus is on determining which model comes closest to the observed data and if there are statistical differences in model predictions in low wind speed conditions.

# CHAPTER 3

# METHODOLOGY

## General Perspective

The focus of this experiment is on the behavior of gaseous plumes under low wind speed conditions. This information is important since it is believed that many plume models generally over-estimate plume concentration in weak winds. This quantitative research is designed to determine the plume behavior of a representative set of three gasses in low wind speed conditions. The gasses used in this experiment are ammonia, for buoyant gas analysis; ethylene, for neutral buoyancy gas analysis; and propylene, for dense gas analysis. The selection of these three gasses is based on their relatively low cost, ease of handling, and, most importantly, the ability of our instruments (i.e., Photoionization Detectors [PIDs]), to identify airborne concentration levels.

## Research Context and Participants

This quantitative research consists of a series of experiments that generate plume concentration data in low wind speed conditions for comparison against model predictions of plume concentrations from three commercial dispersion models. The objective of this research is to determine which of the three models best matches the

measured data and to determine any commonalities between the observed data and the model predictions. Statistical analysis will be used to determine model bias and scatter.

The participants in this experiment include the Principal Investigators, Dr. Richard Venedam and Patrick Sawyer of National Security Technologies, LLC (NSTec), Test and Evaluation Department; Dr. Kevin Kyle from DOE's Special Technologies Laboratory in Santa Barbara, and the NSTec technical staff of the Nonproliferation Test and Evaluation Complex (NPTEC) at the NTS.

## Instruments and Procedures Used in Data Collection

Three types of data were collected during this experiment. Meteorological data were collected by the NPTEC staff, including wind speed, wind direction, temperature, barometric pressure, and humidity. The second type of data is chemical release data, specifically source flow rates collected by the release system process control computer operated by the NPTEC staff. The third type of data collected is chemical plume concentration data collected by PIDs, operated by Dr. Kyle.

PIDs are instruments that ionize a sample of gas using an ultraviolet (uv) lamp. The ionized gas molecules then flow across a charged plate that separates the positive from the negative ions and produces a current. The measured current is a function of the concentration of the ionized species in the gas sample. The output is a digital readout of the parts per million (ppm) or the parts per billion (ppb) concentration of the species. For this experiment, 35 of the 36 PIDs measure concentrations in the ppb range; one PID, located on the innermost ring, measures concentrations in the ppm range.

PIDs will ionize any gas with an ionization potential (IP) below the output of the lamp. Most commercial PIDs come with 9.8, 10.6, or 11.7 electronvolt (eV) ratings. All compounds can be ionized, but they differ in the amount of energy required to displace an electron or ionize the compound. This value is called the IP of the compound. IP is a measure of the bond strength of a compound. If the IP is greater than that of air, then a PID will not produce useful information since, the air molecules themselves will be ionized and produce a false signal. Fortunately, most organic compounds ionize at levels below that of air. Ionization energies for the chemicals of interest are ammonia at 10.16 eV, ethylene at 10.51 eV, and propylene at 9.73 eV. The PIDs used for these experiments all have a lamp rating of 10.6 eV. The PIDs were mounted on tripods with their inlets at 2 m above ground level.

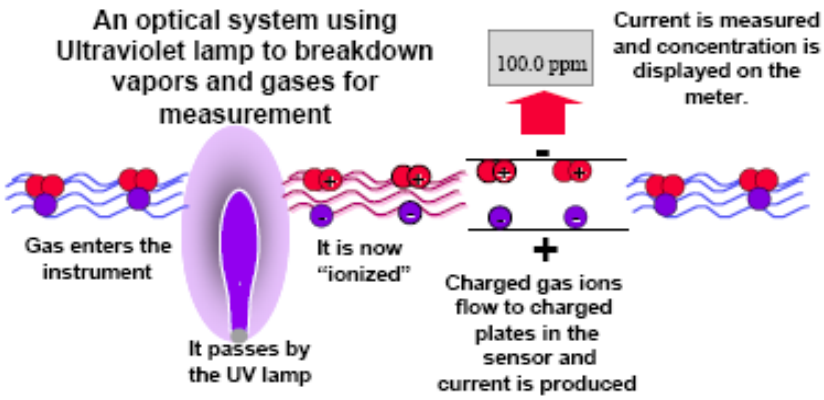


http://www.conceptcontrols.com/app-tech-notes/rae_tech/AP-000%20%20v2%20RAE%20PID%20Training%20Outline.pdf

*Figure 3 Photoionization Schematic*


*Figure 4 Rae PID with radio frequency (RF) Transmitter*

The Rae Systems PID sensors require a two point calibration to correctly define the sensor calibration curve. A zero point calibration is performed using a charcoal filter to remove organic vapors from ambient air. The filters are a standard item supplied by Rae Systems. The second point of the calibration curve is the span calibration provided by reference gas in zero air. The gas provided by RAE Systems is isobutylene (10 ppm for the ppbRAE, and 100 ppm for the MiniRAE 2000). The span gas is delivered to the PID at 500 milliliters per minute through a flow-limiting regulator, or alternatively through a flow-demand regulator. Values thus obtained are stored in the PID electronic memory and applied to all subsequent raw lamp current readings. Concentrations of test gasses, propylene, ethylene, and ammonia, are determined by applying a proportionality factor, or correction factor to the PID readings. For this test series, the PIDs were calibrated and checked approximately one week before the releases. Past experience in the field has shown that the PIDs will hold their calibrations over a period of months or longer. The exception to this is when the PIDs are subjected to vapors that may leave residue on the sensing electrodes. The current suite of gasses does not fall into this category. The PIDs

use a dual channel sensing structure to compensate for variations in lamp intensity. One channel measures a current due to ionized gas, while the second channel measures a current due to ionized gas and photoelectric emission of electrons from the metal electrode surface, which is a function of the UV (10.6 eV) lamp intensity.

Meteorological data was collected by a Vaisala WXT510 weather transmitter, co-located with the source, and eight Vaisala WS425 ultrasonic wind sensors arranged in a grid pattern surrounding the 100 m circle. The WXT510 provides wind speed and direction, barometric pressure, temperature, and relative humidity. The WS425 sensors provides wind speed and direction. The wind sensors were fixed 2 m above the ground.


*Figure 5* *Vaisala WS425 Ultrasonic Wind Sensor*

The experiments are divided into three sets, one for each chemical. Ammonia and ethylene were released five times for 5 min each, to represent puff releases, and five times for 20 min each to represent plume releases. Propylene was released a total of twelve times (five 5 min puffs, six 20 min plumes, and a single 30 min plume). There was a brief time period between each release to allow for the area to clear of any residual

chemical and for the PIDs to reset. The ammonia releases are limited based on the zero wind constraints specified in the environmental assessment for chemical releases at the NTS, DOE/EA-1494.

Figure 6 shows the release point. The box contains the release control equipment and the pole adjacent to the box is the RF link that allows remote operation of the system. Portions of the PID array can also be seen in this photo. The tower in the middle supports the release tubes which are situated exactly 2 m above ground. A three-dimensional wind sensor is mounted at the top of the 10 m tower to provide information on the vertical wind direction component.


*Figure 6 Release Apparatus Setup*

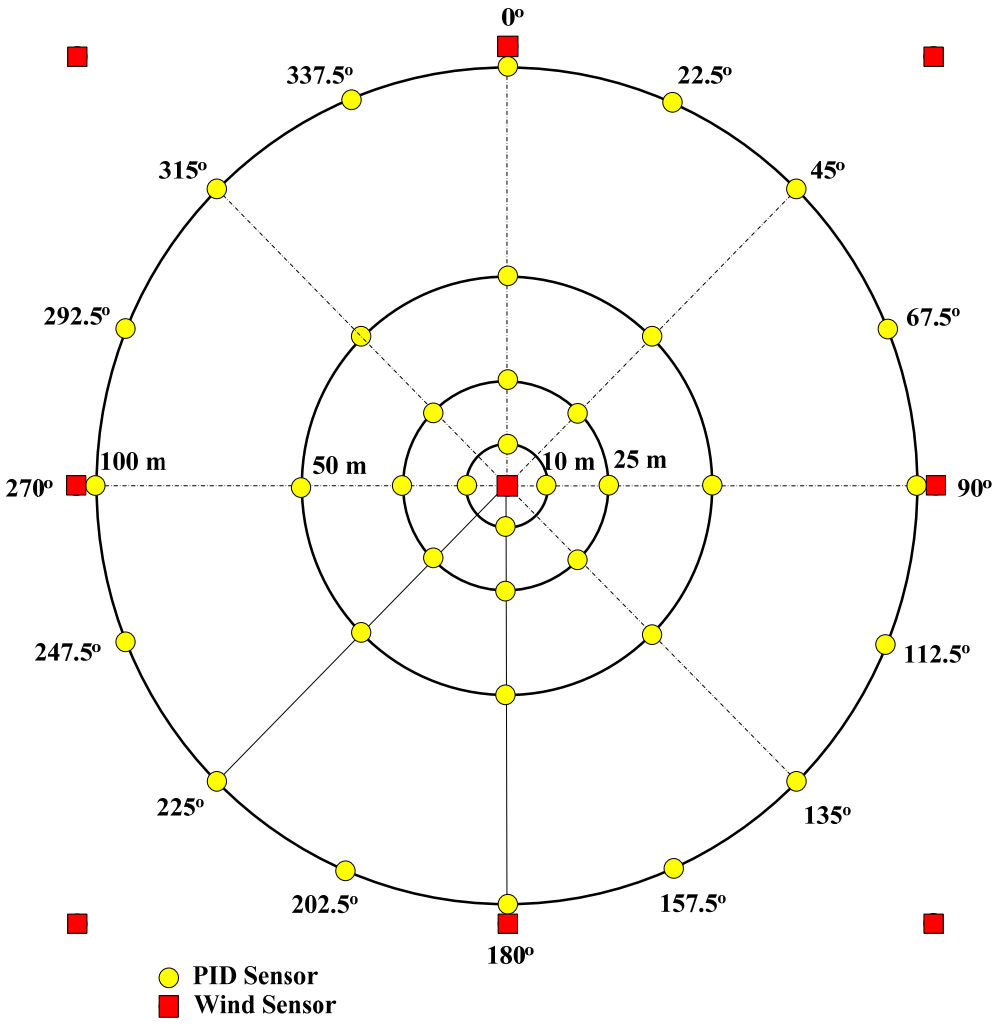


Figure 7 Sensor Array

The sensor array consists of 36 PIDs positioned in four circles. The inner circle, 10 m from the release source, contains four PIDs. The second circle, 25 m from the release source, contains 8 PIDs. The third circle, 50 m from the release source, contains eight PIDs. The fourth circle, 100 m from the release source, contains sixteen PIDs. Nine wind sensors are included in the array, one co-located with the source and eight arranged in a grid surrounding the PID array.

Most of the releases were conducted when the prevailing wind speed was below 2 m/s. In eight of ten ammonia releases, eight of ten ethylene releases, and eleven of twelve propylene releases, the mean wind speed over the duration of the release was below 2 m/s.

## Data Analysis

Data generated during this experiment is divided into two groups: observed data measured by instrumentation in the field and predicted data generated from model outputs. Experiments were conducted at different source strengths to determine if model predictions have a correlation to source strength. Since models treat puffs and continuous plumes differently, each set of different source strengths were released over two time periods: 5 min durations to produce puff data and 20 min durations to generate continuous plume data. Since time allowed, an additional 20 min low rate propylene release was conducted to make up for the lack of data on an earlier propylene release. On the final day of releases, a 30 min release of propylene was conducted to obtain additional data.

The data generated is analyzed in accordance with American Society of Testing Materials (ASTM) Standard D6589-05, Standard Guide for Statistical Evaluation of Atmospheric Dispersion Model Performance. The primary goal of the statistical evaluation is to test the null hypothesis: Gaussian atmospheric dispersion models underestimate peak plume concentrations in low wind conditions. A secondary goal of the analysis is to determine which of the three models tested best matches the observed

data. The second objective is obtained using statistical evaluation to determine which of the models contains the smallest bias and scatter in comparison with observations.

The initial data analysis looks at all the observed concentrations versus the model-predicted concentrations. These data are analyzed using a scatter plot to determine relative over-prediction or under-prediction in the models. A scatter plot also shows the scatter of the data sets between the models.

The FAC2 analysis shows the number of predictions within a factor of two of the observations. Chang and Hanna (2004) note that a FAC2 of greater than 0.5 is representative of a "good" model (for wind speeds over 2 m/s).

## Summary of the Methodology and Time Line

The goal of this experiment is to collect data that is used to compare how well three atmospheric plume dispersion models predict downwind plume concentrations versus observed plume concentrations. Data were collected from the release of three chemicals representing buoyant gas (ammonia), neutral buoyancy gas (ethylene), and heavier than air gas (propylene). The data will be shared with the scientific community in order to enhance the effectiveness of plume dispersion model algorithms used to determine diffusion coefficients in low wind conditions.

These experiments were conducted on February 13, 15, and 16, 2007 at NPTEC located on the Frenchman Flat dry lake bed at the NTS.

# CHAPTER 4

# FINDINGS OF THE STUDY

A total of 32 data sets were obtained from the release experiments. Two sets of data were not considered for further analysis due to zero readings from the PIDs. Factors such as a narrow plume width, meander, and loft can result in plumes missing detectors in the grid. To limit the lofting due to the high flow rates associated with the ethylene and propylene releases, a deflector plate was installed above the release tubes. This plate reduced the vertical velocity component at the release point, reducing the chance that the plume would carry over the PID array.

## Data Description

Flow rates and weather data were recorded every 2 sec. The mean value of the 2 sec flow rate data was averaged over the entire period of the release to generate the flow rate observation used in the model inputs. Similarly, for the wind speed and direction data, the output from the eight WS425 sensors was averaged over the period of release to generate a mean wind speed and mean wind direction for model input.

PID concentration data are collected every 4 sec. The PIDs collected readings after the source stopped releasing as the plume slowly made its way downwind. The

highest observed 2 min average concentration on each of the four PID rings is used as the observed concentration ($C_o$). This will be compared against the time averaged plume centerline predicted concentration ($C_p$) from the models. The SCIPUFF model output shows instantaneous concentrations at specific times at the receptor locations. The highest 2 min average concentration was used for $C_p$.

Stability class is determined using the standard deviation of the wind direction during the release period ($\sigma_\theta$). The $\sigma_\theta$ from each of the eight WS425 sensors was calculated and the mean $\sigma_\theta$ was used to determine the stability class for each release using the following criteria (Hanna, 1983):

| Stability Class | Standard Deviation of Wind Direction ($\sigma_\theta$) |
|---|---|
| A | $\geq 22.5^o$ |
| B | $17.5^o$ to $22.5^o$ |
| C | $12.5^o$ to $17.5^o$ |
| D | $7.5^o$ to $12.5^o$ |
| E | $3.8^o$ to $7.5^o$ |
| F | $< 3.8^o$ |

In the early 1980s, the Desert Tortoise and Goldfish experiments produced surface roughness length estimates of 0.0002 and 0.003 m (Hanna et al., 1993). Wieringa (1993) recommends a $z_o$ of 0.0003 m for terrain similar to the NPTEC facility, which sits on a dry lake bed with a mostly hard clay surface. The 0.0003 m value was used for the model input.

Each of the three models has their own unique set of data inputs. Tables 1A through 1C list the inputs used to generate the model predictions.

Table 1A ALOHA Model Inputs

| Variable | Model Input |
|---|---|
| Release Chemical | Chemical selected from model library |
| Wind Speed (m/s)[1] | Mean wind speed calculated for each release |
| Wind Speed Height (m) | 2.0 |
| Surface Roughness (cm) | 0.03 |
| Cloud Cover (percent [%]) | 30 |
| Air Temperature ($^{o}$C) | Mean temperature calculated for each release |
| Stability Class (A-F)[1] | Determined for each release based on $\sigma_\theta$ calculation |
| Humidity (%) | Mean humidity calculated for each release |
| Release Rate (kg/hr) | Mean source rate calculated for each release |
| Length of Run (min) | Actual release time for each run |
| Source Height (m) | 2.0 |

1 ALOHA will force values for minimum wind speed and stability class based on user inputs. This was frequently the case for these model runs, resulting in an ALOHA wind speed in excess of the actual wind speed.

Table 1B EPIcode Model Inputs

| Variable | Model Input |
|---|---|
| Release Type: Continuous or Term | Continuous |
| Release Chemical | Chemical selected from model library |
| Release Rate (kg/hr) | Mean source rate calculated for each release |
| Effective Release Height (m) | 2.0 |
| 2 Meter Wind Speed (m/s) | Mean wind speed calculated for each release |
| Airborne Fraction | 1.0 |
| Wind Input Height (m) | 2.0 |
| Deposition Velocity (cm/s) | 0.0 |
| Stability Class (A-F) | Determined for each release based on $\sigma_\theta$ calculation |
| Terrain: Standard (Conservative) or Urban | Standard |
| Max Sample Time (min) | 2.0 |
| Source Altitude MSL (m) | 1,000 |
| Source Geometry: Simple or Complex | Simple |

Table 1C SCIPUFF Model Inputs

| Variable | Model Input |
|---|---|
| Mode | Source Contribution |
| Release AGL (m) | 2.0 |
| Max Time Step (sec) | 4.0 |
| Period – Start Date/Time and End Date/Time | Actual Release date and time |
| Domain (Latitude/Longitude) | Actual GPS coordinates of 200 m x 200 m box surrounding the sensor array |
| Materials | User created library including density, deposition velocity, and mole weight for each chemical |
| Met Data | Fixed |
| Wind Speed (m/s) | Mean wind speed calculated for each release |
| Release Type | Continuous |
| Location | GPS coordinates of release point |
| Emission Rate (kg/sec) | Mean source rate calculated for each release |
| $\sigma_y$ (m) | 1.0 (Based on estimated Plume width at source prior to advection) |
| $\sigma_z$ (m)[1] | 1.0 for Q <6.0 kg/hr, 2.0 for 6.0 < Q < 11 kg/hr and 3.0 for Q > 11 kg/hr |
| Release Duration (min) | Actual release time for each run |

1 The $\sigma_z$ dispersion coefficient at the source is difficult to estimate due to jet effects of the chemical being released through the ¾ inch diameter tube. The higher vertical component, $\sigma_z$, is due to the increased exit velocity of the chemical at higher mass flow rates. The dispersion coefficients used for the model input are based upon estimates of the size and shape of the plume prior to advection carrying the plume down range where it disburses in a Gaussian manner.

## Experimental Observations

Data for the chemical releases are shown below in tables 2A, 3A, and 4A for ammonia, ethylene, and propylene respectively. The observed 2 min average PID and model-predicted centerline concentrations are shown in tables 2B, 3B, and 4B respectively.

Table 2A Ammonia Experiment (Measured Data)

| Ammonia Experiment | Release | | | | | | | | | |
|---|---|---|---|---|---|---|---|---|---|---|
| | 1 | 2 | 3 | 4 | 5 | 6 | 7 | 8 | 9 | 10 |
| Mean Flow Rate (kg/hr) | 0.73 | 0.49 | 1.10 | 1.54 | 2.04 | 0.68 | 2.02 | 1.65 | 1.03 | 0.76 |
| Mean Temperature ($^{o}$C) | 1.26 | 1.44 | 2.05 | 2.27 | 2.33 | 3.38 | 5.33 | 7.00 | 8.29 | 9.10 |
| Average Wind Speed (m/s) | 1.46 | 1.21 | 0.88 | 1.20 | 0.80 | 0.75 | 0.74 | 1.59 | 2.16 | 2.60 |
| Average Wind Direction ($^{o}$N) | 40.76 | 97.98 | 80.10 | 63.68 | 67.85 | 186.33 | 198.86 | 162.53 | 208.03 | 236.34 |
| Avg Wind Speed Std Dev ($\sigma_v$) | 0.29 | 0.39 | 0.27 | 0.23 | 0.21 | 0.33 | 0.44 | 0.38 | 0.59 | 0.55 |
| Avg Wind Dir Std Dev ($\sigma_\theta$) | 25.23 | 15.66 | 14.91 | 17.30 | 18.04 | 110.02 | 70.19 | 21.25 | 19.13 | 11.52 |
| Stability Class | A | C | C | C | B | A | A | B | B | D |
| Avg Wind Pitch Std Dev ($\sigma_z$) | 3.56 | 2.34 | 3.37 | 5.77 | 5.60 | 20.79 | 33.02 | 13.68 | 8.90 | 10.45 |
| Surface Roughness Length ($z_o$) | 0.0003 | 0.0003 | 0.0003 | 0.0003 | 0.0003 | 0.0003 | 0.0003 | 0.0003 | 0.0003 | 0.0003 |
| Run Time (min) | 0:07:06 | 0:05:00 | 0:05:04 | 0:04:56 | 0:04:58 | 0:20:00 | 0:20:02 | 0:20:00 | 0:20:02 | 0:20:02 |

Table 2B Ammonia Experiment (Observed and Predicted Concentrations)

| Release | 1 | 2 | 3 | 4 | 5 | 6 | 7 | 8 | 9 | 10 |
|---|---|---|---|---|---|---|---|---|---|---|
| PID Observations (Highest 2 min average on each ring) | | | | | | | | | | |
| 2 Min Avg 10 m $C_o$ (ppm) | 27.79 | 121.31 | 35.13 | 57.42 | 72.81 | 25.782 | 35.846 | 45.621 | 8.545 | 0.886 |
| 2 Min Avg 25 m $C_o$ (ppm) | 55.881 | 35.09 | 11.21 | 18.84 | 2.01 | 7.686 | 7.93 | 2.644 | 4.841 | 4.08 |
| 2 Min Avg 50 m $C_o$ (ppm) | 8.977 | 23.70 | 0.00 | 5.8 | 3.84 | 1.7 | 0.304 | 0.406 | 1.971 | 1.857 |
| 2 Min Avg 100 m $C_o$ (ppm) | 0.911 | 5.22 | 0.13 | 2.5 | 4.31 | 2.73 | 0.078 | 0.039 | 0.144 | 0.022 |
| ALOHA Predictions | | | | | | | | | | |
| Centerline 10 m $C_p$ (ppm) | 7.83 | 2.28 | 6.89 | 7.24 | 33.2 | 11.8 | 35.3 | 15.6 | 7.21 | 0.251 |
| Centerline 25 m $C_p$ (ppm) | 1.91 | 5.06 | 15.3 | 16.1 | 17.1 | 2.87 | 8.6 | 8.03 | 3.71 | 4.54 |
| Centerline 50 m $C_p$ (ppm) | 0.507 | 1.85 | 5.6 | 5.88 | 5.04 | 0.764 | 2.29 | 2.37 | 1.1 | 2.29 |
| Centerline 100 m $C_p$ (ppm) | 0.129 | 0.512 | 1.55 | 1.63 | 1.32 | 0.194 | 0.581 | 0.62 | 0.286 | 0.708 |
| EPIcode Predictions | | | | | | | | | | |
| Centerline 10 m $C_p$ (ppm) | 11.00 | 40.00 | 120.00 | 130.00 | 120.00 | 20.00 | 62.00 | 48.00 | 22.00 | 54.00 |
| Centerline 25 m $C_p$ (ppm) | 2.80 | 7.30 | 23.00 | 23.00 | 26.00 | 5.0 | 15 | 11 | 4.9 | 8.9 |
| Centerline 50 m $C_p$ (ppm) | 0.77 | 2.60 | 8.00 | 8.2 | 8.4 | 1.4 | 4.2 | 3.4 | 1.6 | 3.1 |
| Centerline 100 m $C_p$ (ppm) | 0.20 | 0.77 | 2.4 | 2.4 | 2.3 | 0.36 | 1.1 | 0.93 | 0.43 | 1.0 |
| SCIPUFF Predictions | | | | | | | | | | |
| Centerline 10 m $C_p$ (ppm) | 20.94 | 18.36 | 41.39 | 49.52 | 93.01 | 22 | 62.87 | 53.94 | 29.58 | 14.43 |
| Centerline 25 m $C_p$ (ppm) | 7.67 | 6.01 | 13.46 | 17.76 | 26.58 | 7.41 | 21.07 | 20.95 | 10.87 | 8.1 |
| Centerline 50 m $C_p$ (ppm) | 4.18 | 3.02 | 5.75 | 8.7 | 7.47 | 3.7 | 10.96 | 9.01 | 5.37 | 3.88 |
| Centerline 100 m $C_p$ (ppm) | 1.99 | 1.39 | 1.23 | 2.61 | 1.27 | 1.48 | 4.14 | 5.27 | 2.97 | 2.11 |

Table 3A Ethylene Experiment (Measured Data)

| Ethylene Experiment | Release | | | | | | | | |
|---|---|---|---|---|---|---|---|---|---|
| | 1 | 2 | 3 | 4 | 6 | 7 | 8 | 9 | 10 |
| Mean Flow Rate (kg/hr) | 1.00 | 2.00 | 4.83 | 10.42 | 1.01 | 2.00 | 5.07 | 10.27 | 19.74 |
| Mean Temperature ($^{o}$C) | 3.12 | 3.59 | 3.77 | 3.77 | 3.76 | 3.76 | 3.77 | 3.77 | 3.77 |
| Average Wind Speed (m/s) | 1.54 | 1.53 | 1.86 | 2.22 | 1.13 | 1.17 | 1.14 | 1.50 | 1.12 |
| Average Wind Direction ($^{o}$N) | 199.16 | 158.98 | 96.73 | 92.68 | 142.50 | 96.31 | 242.91 | 217.60 | 150.65 |
| Avg Wind Speed Std Dev ($\sigma_v$) | 0.56 | 0.44 | 0.29 | 0.49 | 0.37 | 0.32 | 0.51 | 0.51 | 0.46 |
| Avg Wind Dir Std Dev ($\sigma_\theta$) | 20.64 | 8.03 | 8.32 | 8.96 | 29.21 | 26.19 | 41.49 | 24.97 | 40.47 |
| Stability Class | B | D | D | D | A | A | A | A | A |
| Avg Wind Pitch Std Dev ($\sigma_z$) | 5.04 | 5.31 | 6.46 | 6.53 | 8.68 | 10.49 | 16.01 | 12.66 | 17.82 |
| Surface Roughness Length ($z_o$) | 0.0003 | 0.0003 | 0.0003 | 0.0003 | 0.0003 | 0.0003 | 0.0003 | 0.0003 | 0.0003 |
| Run Time (min) | 0:05:00 | 0:04:56 | 0:04:58 | 0:05:02 | 0:19:58 | 0:20:02 | 0:20:02 | 0:20:00 | 0:20:00 |

Table 3B Ethylene Experiment (Observed and Predicted Concentrations)

| Release | 1 | 2 | 3 | 4 | 6 | 7 | 8 | 9 | 10 |
|---|---|---|---|---|---|---|---|---|---|
| PID Observations (Highest 2 min average on each ring) | | | | | | | | | |
| 2 Min Avg 10 m $C_o$ (ppm) | 9.083 | 13.55 | 101.85 | 234.871 | 20.502 | 18.414 | 57.77 | 167.782 | 118.977 |
| 2 Min Avg 25 m $C_o$ (ppm) | 1.917 | 0.13 | 29.67 | 101.85 | 6.23 | 4.898 | 13.373 | 54.545 | 70.354 |
| 2 Min Avg 50 m $C_o$ (ppm) | 0.987 | 0.90 | 12.28 | 28.91 | 0.58 | 1.687 | 4.564 | 5.08 | 23.028 |
| 2 Min Avg 100 m $C_o$ (ppm) | 0.197 | 0.70 | 2.44 | 11.108 | 0.488 | 0.16 | 0.499 | 1.785 | 2.438 |
| ALOHA Predictions | | | | | | | | | |
| Centerline 10 m $C_p$ (ppm) | 5.12 | 0.619 | 2.58 | 4.67 | 5.48 | 10.8 | 27.5 | 55.7 | 107 |
| Centerline 25 m $C_p$ (ppm) | 2.63 | 11.2 | 46.7 | 84.4 | 1.33 | 2.64 | 6.7 | 13.6 | 26.1 |
| Centerline 50 m $C_p$ (ppm) | 0.778 | 5.66 | 23.6 | 42.6 | 0.355 | 0.702 | 1.78 | 3.61 | 6.93 |
| Centerline 100 m $C_p$ (ppm) | 0.203 | 1.75 | 7.28 | 13.2 | 0.0902 | 0.179 | 0.453 | 0.917 | 1.76 |
| EPIcode Predictions | | | | | | | | | |
| Centerline 10 m $C_p$ (ppm) | 18 | 150 | 290 | 520 | 12 | 23 | 61 | 94 | 240 |
| Centerline 25 m $C_p$ (ppm) | 4.1 | 24 | 48 | 87 | 3 | 5.7 | 15 | 23 | 59 |
| Centerline 50 m $C_p$ (ppm) | 1.3 | 8.3 | 17 | 30 | 0.83 | 1.6 | 4.1 | 6.4 | 16 |
| Centerline 100 m $C_p$ (ppm) | 0.35 | 2.8 | 5.5 | 9.9 | 0.21 | 0.41 | 1.1 | 1.6 | 4.2 |
| SCIPUFF Predictions | | | | | | | | | |
| Centerline 10 m $C_p$ (ppm) | 19.78 | 30.7 | 54.83 | 114.48 | 20.09 | 39.73 | 71.05 | 118.65 | 249.8 |
| Centerline 25 m $C_p$ (ppm) | 7.57 | 15.18 | 26.47 | 49.88 | 7.11 | 14.03 | 31.06 | 61.63 | 103.37 |
| Centerline 50 m $C_p$ (ppm) | 3.74 | 7.5 | 14.93 | 28.85 | 3.48 | 6.88 | 16.98 | 30.15 | 59.12 |
| Centerline 100 m $C_p$ (ppm) | 1.83 | 3.67 | 8.39 | 16.24 | 1.98 | 3.81 | 9.05 | 17.47 | 29.1 |

Table 4A Propylene Experiment (Measured Data)

| Propylene Experiment | Release | | | | | | | | | | |
|---|---|---|---|---|---|---|---|---|---|---|---|
| | 1 | 2 | 4 | 5 | 6 | 7 | 8 | 9 | 10 | 6B | Bonus |
| Mean Flow Rate (kg/hr) | 1.00 | 2.00 | 9.80 | 19.39 | 1.03 | 2.04 | 5.18 | 10.16 | 19.76 | 1.28 | 1.04 |
| Mean Temperature ($^{o}$C) | 14.00 | 13.92 | 3.77 | 3.77 | 5.00 | 2.68 | 3.77 | 16.12 | 14.81 | 0.73 | 6.20 |
| Average Wind Speed (m/s) | 1.42 | 1.79 | 1.35 | 1.48 | 1.62 | 1.64 | 1.84 | 1.63 | 1.27 | 1.98 | 1.38 |
| Average Wind Direction ($^{o}$N) | 240.72 | 269.60 | 173.49 | 147.49 | 98.21 | 64.53 | 163.20 | 193.27 | 207.51 | 104.44 | 139.29 |
| Avg Wind Speed Std Dev ($\sigma_v$) | 0.40 | 0.39 | 0.46 | 0.48 | 0.90 | 0.41 | 0.41 | 0.31 | 0.29 | 0.48 | 0.52 |
| Avg Wind Dir Std Dev ($\sigma_\theta$) | 22.74 | 29.68 | 16.12 | 16.08 | 34.90 | 17.57 | 12.78 | 18.53 | 19.61 | 101.10 | 22.47 |
| Stability Class | A | A | C | C | A | B | C | B | B | A | B |
| Avg Wind Pitch Std Dev ($\sigma_z$) | 6.49 | 6.93 | 10.46 | 12.20 | 10.44 | 1.76 | 6.17 | 2.54 | 2.94 | 2.27 | 8.75 |
| Surface Roughness Length ($z_o$) | 0.0003 | 0.0003 | 0.0003 | 0.0003 | 0.0003 | 0.0003 | 0.0003 | 0.0003 | 0.0003 | 0.0003 | 0.0003 |
| Run Time (min) | 0:05:00 | 0:04:58 | 0:04:58 | 0:04:54 | 0:20:56 | 0:20:58 | 0:20:00 | 0:19:56 | 0:19:56 | 0:20:14 | 0:30:04 |

Table 4B Propylene Experiment (Observed and Predicted Concentrations)

| Release | 1 | 2 | 4 | 5 | 6 | 7 | 8 | 9 | 10 | 6B | Bonus |
|---|---|---|---|---|---|---|---|---|---|---|---|
| PID Observations (Highest 2 min average on each ring) | | | | | | | | | | | |
| 2 Min Avg 10 m $C_o$ (ppm) | 3.324 | 0.16 | 69.681 | 30.17 | 11.161 | 28.127 | 52.91 | 107.911 | 5.886 | 66.904 | 10.639 |
| 2 Min Avg 25 m $C_o$ (ppm) | 4.934 | 2.66 | 20.34 | 28.44 | 4.391 | 4.445 | 22.724 | 43.11 | 37.701 | 12.397 | 6.22 |
| 2 Min Avg 50 m $C_o$ (ppm) | 3.85 | 0.76 | 2.97 | 8.012 | 0.355 | 1.114 | 6.113 | 11.735 | 15.871 | 4.82 | 0.196 |
| 2 Min Avg 100 m $C_o$ (ppm) | 1.759 | 0.19 | 0.271 | 5.283 | 2.134 | 5.033 | 3.526 | 20.851 | 29.054 | 2.408 | 1.992 |
| ALOHA Predictions | | | | | | | | | | | |
| Centerline 10 m $C_p$ (ppm) | 3.75 | 14.4 | 12.9 | 25.6 | 3.74 | 6.95 | 12.6 | 36.3 | 70.3 | 7.95 | 3.59 |
| Centerline 25 m $C_p$ (ppm) | 0.913 | 3.51 | 28.7 | 56.9 | 0.911 | 3.57 | 27.9 | 18.7 | 36.1 | 1.94 | 1.84 |
| Centerline 50 m $C_p$ (ppm) | 0.243 | 0.933 | 10.5 | 20.8 | 0.242 | 1.06 | 10.2 | 5.52 | 10.7 | 0.515 | 0.546 |
| Centerline 100 m $C_p$ (ppm) | 0.0618 | 0.237 | 2.91 | 5.75 | 0.0616 | 0.276 | 2.82 | 1.44 | 2.79 | 0.131 | 0.143 |
| EPIcode Predictions | | | | | | | | | | | |
| Centerline 10 m $C_p$ (ppm) | 6.4 | 10 | 290 | 530 | 5.8 | 23 | 110 | 120 | 290 | 5.9 | 14 |
| Centerline 25 m $C_p$ (ppm) | 1.6 | 2.5 | 53 | 96 | 1.4 | 5.2 | 21 | 26 | 65 | 1.4 | 3.1 |
| Centerline 50 m $C_p$ (ppm) | 0.44 | 0.69 | 19 | 34 | 0.39 | 1.7 | 7.3 | 8.3 | 21 | 0.4 | 1.0 |
| Centerline 100 m $C_p$ (ppm) | 0.11 | 1.8 | 5.6 | 10 | 0.1 | 0.45 | 2.2 | 2.2 | 5.6 | 0.01 | 0.27 |
| SCIPUFF Predictions | | | | | | | | | | | |
| Centerline 10 m $C_p$ (ppm) | 12.83 | 24.97 | 81.75 | 149.8 | 13.18 | 26.38 | 39.39 | 86.94 | 154.5 | 14.78 | 12.98 |
| Centerline 25 m $C_p$ (ppm) | 4.69 | 10.64 | 37.96 | 68.54 | 4.73 | 9.96 | 18.89 | 41.91 | 71.18 | 5.85 | 4.97 |
| Centerline 50 m $C_p$ (ppm) | 2.6 | 4.91 | 21.8 | 36.63 | 2.57 | 4.63 | 10.85 | 23.01 | 41.5 | 2.78 | 2.47 |
| Centerline 100 m $C_p$ (ppm) | 1.35 | 2.54 | 11.27 | 18.29 | 1.35 | 2.69 | 6.09 | 12.84 | 23.06 | 1.51 | 1.4 |

## Statistical Analysis

The simplest method of comparing the models performance with the observed data is a simple scatter plot of the predicted versus observed concentrations.

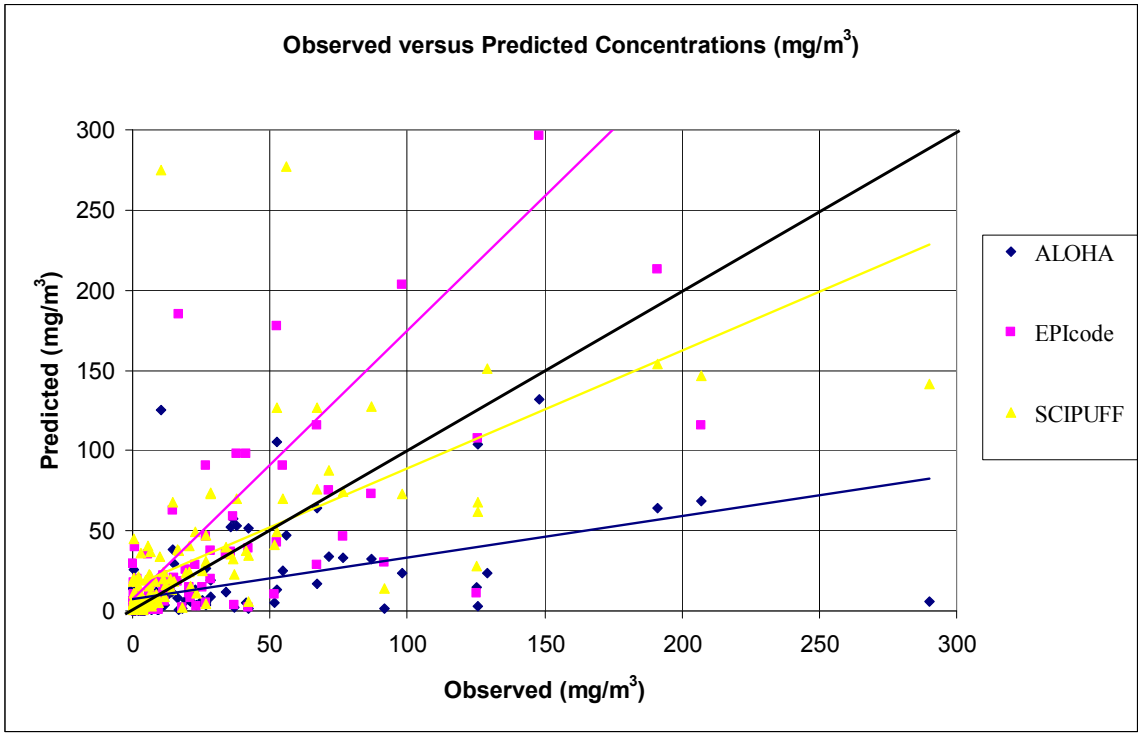


Figure 8 Observed versus Predicted Concentrations

This chart includes trend lines to show the relative over-prediction of the EPIcode data and the relative under-prediction of the ALOHA data. The SCIPUFF trend line indicates relative over-prediction at lower concentrations and relative under-prediction at higher concentrations. The significant scatter in the EPIcode data can also be easily seen.

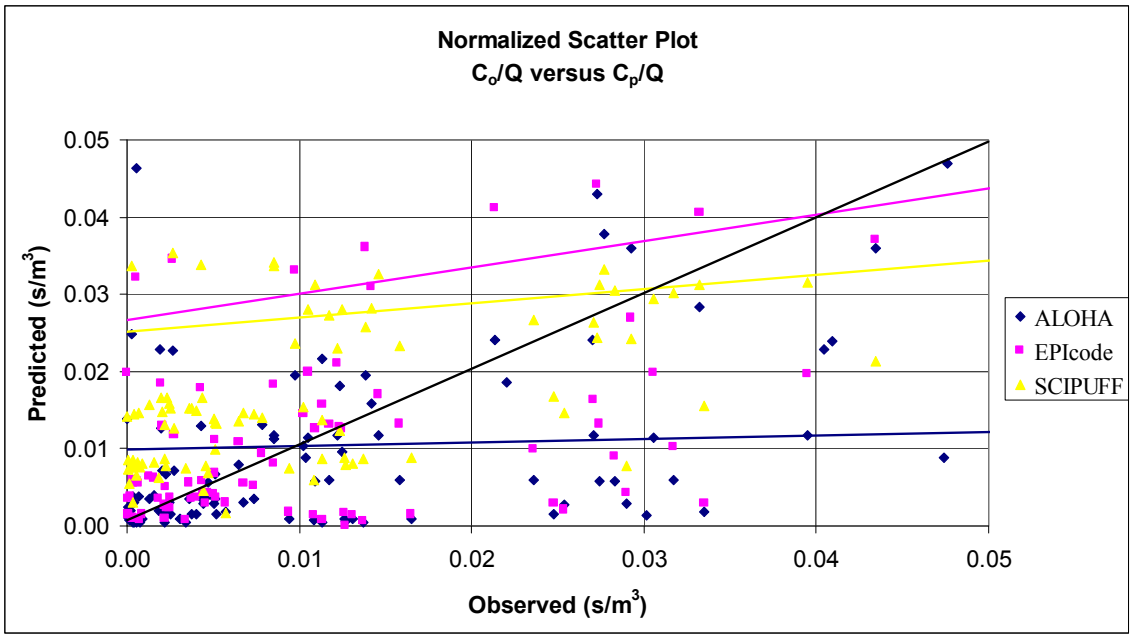


Figure 9 Observed versus Predicted Concentrations (Normalized)

Figure 9 is a scatter plot of the data after it has been normalized by dividing the observed and predicted concentrations by the flow rates for each experiment. The trend lines for all three models are below the 1 to 1 line, indicating general under-prediction, in the region above 0.04 s/m$^3$. Below that normalized value, the EPIcode and SCIPUFF trends are above the 1 to 1 line, indicating general over-prediction, while the ALOHA trend line only exceeds the 1 to 1 line in the region below 0.01 s/m$^3$.

Tables 5 through 9 list the results of the statistical data analysis using the six performance measures recommended by Chang and Hanna (2004). These tables include statistical data broken out into distance from source data, mass flow rate data, chemical species data, and release duration data. All of the data sets have been normalized by dividing the observed and predicted concentrations by the source strength.

Table 5 Overall Model Performance Summary Data

| Factor | Summary | | |
|---|---|---|---|
| | ALOHA | EPIcode | SCIPUFF |
| FAC2 | 0.4000 | 0.4583 | 0.4250 |
| R | 0.0343 | 0.0437 | 0.2099 |
| NMSE | 7.7366 | 4.0864 | 2.2912 |
| FB | 0.8863 | 0.1522 | -0.0694 |
| VG | 25.5082 | 17.4223 | 51.5825 |
| MG | 1.6185 | 0.7093 | 0.4311 |

Table 5 lists the data for the six statistical performance measurements considered for the thirty experiments analyzed. The FAC2 data show all three models are below the 0.5 value considered "good" by Chang and Hanna (2004). However, considering the fact that these data are all at low wind speeds in the near field region, the values of 0.40 to 0.45 should be considered reasonable.

The correlation coefficient is a measure of how well the variables agree with each other. A perfect correlation has an R value of ±1.0, while no correlation between the variables gives an R of 0. All three models have low correlation coefficients with the SCIPUFF predictions showing the highest correlation to the observed data with an R value of 0.2099.

The NMSE indicates the degree of deviation between predicted and observed data. A perfect model will have an NMSE of zero. If the mean value of the predicted data and the mean value of the observed data are the same, then the NMSE would equal 1.0. Using the NMSE performance measure, the SCIPUFF predictions show the closest agreement with the observations, followed by EPIcode and then ALOHA.

FB provides an indication of a models tendency to over-predict or under-predict. Values for FB can range from -2 to 2 with 0 being ideal. ALOHA and EPIcode have positive FB values indicating a bias to under-predict plume concentrations. SCIPUFF, with FB of -0.069, shows a slight bias towards over-prediction. It is worth noting that the FB calculation looks at the mean value of the observed and predicted data, which causes the FB data to favor the higher numbers. This is clearly demonstrated by looking at the EPIcode data. There are 120 pairs of observed-predicted data, and EPIcode over-predicted 72 of those data points and under-predicted 48 data points. This would suggest an over-prediction bias. However, since most of the over-predictions are for low values, when the mean values are taken, the FB shows an under-prediction bias.

VG is a measurement of the mean relative scatter of the data points. SCIPUFF VG data indicate significant scatter among the predicted versus observed data points, while ALOHA shows moderate scatter and EPIcode demonstrates the least amount of relative scatter.

MG measures the relative mean bias of the data with values below 1 indicating an over-prediction bias and values above 1 indicating an under-prediction bias. From the data in Table 5, ALOHA has an under-prediction bias, while EPIcode and SCIPUFF have an over-prediction bias. This is in line with the actual number of over-prediction versus under-prediction data points for the three models. ALOHA under-predicted 79 times and over-predicted 41 times, while SCIPUFF under-predicted 38 times and over-predicted 82 times.

Table 6A 10 Meter and 25 Meter Statistical Data

| Factor | 10 Meter Data | | | 25 Meter Data | | |
|---|---|---|---|---|---|---|
| | ALOHA | EPIcode | SCIPUFF | ALOHA | EPIcode | SCIPUFF |
| FAC2 | 0.2667 | 0.5000 | 0.5667 | 0.5333 | 0.4667 | 0.5000 |
| R | 0.0022 | 0.1481 | 0.3168 | 0.0624 | -0.0029 | 0.0585 |
| NMSE | 10.3759 | 1.9995 | 2.2478 | 4.7908 | 3.2361 | 2.3191 |
| FB | 1.1891 | -1.0709 | 0.1553 | 0.6825 | 0.2560 | 0.1212 |
| VG | 43.7604 | 15.0130 | 7.8671 | 7.2045 | 7.5866 | 6.2641 |
| MG | 2.6528 | 0.4214 | 0.5677 | 1.2392 | 0.8043 | 0.5761 |

Table 6B 50 Meter and 100 Meter Statistical Data

| Factor | 50 Meter Data | | | 100 Meter Data | | |
|---|---|---|---|---|---|---|
| | ALOHA | EPIcode | SCIPUFF | ALOHA | EPIcode | SCIPUFF |
| FAC2 | 0.4667 | 0.6000 | 0.2667 | 0.3333 | 0.2667 | 0.3667 |
| R | 0.1371 | 0.1589 | 0.2820 | -0.0644 | -0.1294 | 0.1824 |
| NMSE | 8.8267 | 6.5179 | 3.4254 | 6.9528 | 4.5920 | 1.1726 |
| FB | 0.6069 | 0.1638 | -0.2742 | 1.0668 | 0.7779 | -0.2800 |
| VG | 8.5864 | 7.1167 | 19.3774 | 42.4816 | 39.9731 | 172.8215 |
| MG | 1.1593 | 0.7709 | 0.3429 | 1.4227 | 1.4227 | 0.2377 |

Tables 6A and 6B show the relationship of model performance versus the distance from the release point. Looking at the FAC2 data, ALOHA predictions are in closest agreement with observations at the 25 m distance, while EPIcode is closest to observations at the 50 m distance and SCIPUFF is in closest agreement at the 10 m distance. ALOHA and EPIcode demonstrate reduced agreement with observed data at the 100 m distance.

The correlation (R) data indicate the ALOHA and EPIcode model predictions more closely correlate to the observed data at the 25 and 50 m distances and less closely

correlate at the 10 m and 100 m distances. The SCIPUFF predictions most closely correlate to the observations at the 10 m distance, followed by the 50 m, 100 m, and finally the 25 meter distance observations.

For ALOHA, the NMSE data for the effect of distance show the least amount of scatter on the 25 and 100 m rings, followed by the 50 m and, finally, the 10 m rings. EPIcode shows the least variability on the 10 m ring followed by the 25 m data, 100 m data, and, finally, the 50 m data. The SCIPUFF data on the 100 m ring shows the least deviation, followed by the 10 m, 25 m, and, finally, the 50 m data.

The FB data for ALOHA shows an under-prediction bias at the 50 and 25 m locations, followed by a slightly greater under-prediction bias at the 100 m distance and the 10 m distance. EPIcode shows slight under-prediction bias at the 25 and 50 m distances, a significant over-prediction bias at the 10 m distance, and a moderate under-prediction bias at the 100 m distance. SCIPUFF shows an over-prediction bias at the 50 m and 100 m distances and an under-prediction bias at the 10 and 25 m distances.

The VG data are consistent for ALOHA and EPIcode models showing the least amount of relative mean scatter at the 25 m or 50 m distances, followed by the 10 m and the 100 meter distance. SCIPUFF shows the least scatter at the 10 and 25 m distances, slightly larger scatter at the 50 m distance, and a significantly large scatter at the 100 m distance. This jump in scatter between the 50 m and 100 m distances is likely the result of the increased density of sensors on the 50 m ring compared to the 100 m ring.

The MG data correlation for distance downwind show that ALOHA has the lowest mean bias at the 50 m distance, followed by slightly more bias at the 25 and 100 m distances and significantly more bias at the 10 m distance. All the ALOHA MG data

indicate an under-prediction of the data. EPIcode shows an over-prediction bias at the 10, 25, and 50 m distances and a moderate under-prediction bias at the 100 m distance. All the SCIPUFF MG data indicate an over-prediction bias at all four distances. The 25 and 10 m distances for the SCIPUFF data show the highest over-prediction bias, while the 50 and 100 m distances show the least over-prediction bias.

Table 7 Mass Flow Rate Statistical Data

| Factor | Low Flow (< 2 kg/hr) | | | High Flow (> 2 kg/hr) | | |
|---|---|---|---|---|---|---|
| | ALOHA | EPIcode | SCIPUFF | ALOHA | EPIcode | SCIPUFF |
| FAC2 | 0.3500 | 0.3875 | 0.3750 | 0.5250 | 0.6000 | 0.5250 |
| R | 0.0454 | 0.0255 | -0.1857 | 0.2537 | 0.2649 | 0.3148 |
| NMSE | 4.6080 | 2.8590 | 1.8333 | 1.8165 | 1.4247 | 0.8758 |
| FB | 0.7625 | 0.0784 | -0.2578 | 0.4053 | -0.4579 | -0.4573 |
| VG | 42.2914 | 36.8833 | 105.8758 | 21.0150 | 6.8686 | 13.0240 |
| MG | 1.5960 | 0.7191 | 0.3890 | 1.6758 | 0.6942 | 0.5207 |

Table 7 shows the relationship of how well the models perform versus the mass flow rate of the chemical. There were 10 data sets for the high flow case and 20 data sets for the low flow case. The FAC2 data demonstrate that the higher flow rates result in better model agreement with observation. This makes sense given the increased likelihood that the sensor array has a higher probability of hits at higher flow rates.

The correlation between the observed and predicted values shows a significant difference associated with the mass flow rate. The high flow R data for ALOHA and EPIcode are an order of magnitude higher than the low flow R data, indicating the predicted values show in much better agreement with observation at the high flow rates.

The SCIPUFF correlation data also indicate a significant bias in favor of higher flow rates with the SCIPUFF R value at high flows twice that of the low flow R value.

As with the FAC2 and R data, the high flow rate NMSE data show significantly less deviation with the observed data compared to the low flow rate NMSE data. Between the three models, SCIPUFF shows the least deviation for both low and high flow rates, followed by EPIcode and, finally, ALOHA.

The FB data for ALOHA indicate a doubling in under-prediction with smaller flow rates. The FB data for EPIcode show a moderate over-prediction at high flow rates and a slight under-prediction at low flow rates. SCIPUFF FB data indicate a doubling of the over-prediction bias at high flow rates.

The VG data for mass flow rate correlation indicates a significant difference in the relative mean scatter of the data. The high flow rate shows much lower relative mean scatter than the low flow rates. This can also be explained by the fact that the higher flow rates will tend to result in more detections on the receptor rings, while the lower flow rates are more hit and miss.

The MG data correlation for mass flow rate indicate a slight increase in geometric mean bias at higher flow rates compared to lower flow rates for ALOHA and SCIPUFF. EPIcode MG data show little difference between the high and low flow rates. Of the three models, SCIPUFF shows the closest correlation to the observed data with a slight over-prediction bias, followed by EPIcode with a slightly greater over-prediction bias and, finally, ALOHA with a significant under-prediction bias.

Table 8A Chemical Species Statistical Data for Ammonia and Ethylene

| Factor | Ammonia | | | Ethylene | | |
|---|---|---|---|---|---|---|
| | ALOHA | EPIcode | SCIPUFF | ALOHA | EPIcode | SCIPUFF |
| FAC2 | 0.3250 | 0.3500 | 0.3750 | 0.5278 | 0.6389 | 0.3056 |
| R | 0.0540 | 0.1326 | 0.0153 | 0.3576 | 0.2725 | -0.4218 |
| NMSE | 10.6249 | 4.8027 | 3.4885 | 1.3730 | 1.4731 | 1.4731 |
| FB | 1.0912 | 0.4697 | 0.2864 | 0.1695 | -0.6766 | -0.6938 |
| VG | 54.7620 | 63.4621 | 757.9715 | 33.8429 | 8.1685 | 31.1942 |
| MG | 1.6915 | 0.6618 | 0.5153 | 2.1374 | 0.6351 | 0.4235 |

Table 8B Chemical Species Statistical Data for Propylene

| Factor | Propylene | | |
|---|---|---|---|
| | ALOHA | EPIcode | SCIPUFF |
| FAC2 | 0.3636 | 0.4091 | 0.5682 |
| R | -0.1215 | -0.4763 | 0.3103 |
| NMSE | 4.8012 | 2.7143 | 0.8524 |
| FB | 0.9043 | 0.3831 | -0.1505 |
| VG | 84.4430 | 73.6898 | 28.7092 |
| MG | 1.8654 | 1.0443 | 0.4360 |

Tables 8A and 8B show the correlation between the chemical species and the model performance. There are 10 data sets for the ammonia, 9 data sets for the ethylene, and 11 data sets for the propylene. The FAC2 data indicates that the ethylene, with a molecular weight close to that of air, had observed and predicted data in closest agreement for the ALOHA and EPIcode models. SCIPUFF FAC2 data indicate closest agreement with propylene observations followed by ammonia and then ethylene. The ALOHA and EPIcode data indicate a possible bias towards neutrally buoyant species. It also indicates that positive buoyant species like ammonia may be difficult to accurately model. It is

interesting to note that SCIPUFF is the only model that does not have an internal chemical data base, and the only input for each chemical was its density and molecular weight.

The R data from all three models show close correlation with ethylene, followed by propylene and then ammonia. This is to be expected given the fact that ethylene is closest to neutral buoyancy and should give the closest correlation between observed and predicted data compared to the dense gas, propylene, and the buoyant gas, ammonia.

The NMSE data also show the least amount of deviation between predicted and observed values for ethylene compared with the ammonia and propylene for ALOHA and EPIcode. SCIPUFF NMSE data indicate the least deviation with the propylene observations, followed by the ethylene and then the ammonia observations. However, the SCIPUFF predictions are relatively consistent when compared to the ALOHA and EPIcode NMSE data.

The FB data for ALOHA indicate the least amount of under-prediction bias with the ethylene data, followed by the propylene and, finally, the ammonia data, matching similar findings in the previous statistical parameters. The EPIcode FB data are interesting in that they indicate a tendency to over-predict ethylene, while very slightly under-predicting the ammonia and propylene concentrations. The FB data for SCIPUFF show a small under-prediction bias with ammonia, followed by a medium over-prediction with propylene and slightly more over-prediction bias with ethylene.

The VG data correlation to chemical species indicate the least amount of relative scatter for ALOHA and EPIcode with ethylene. ALOHA and EPIcode show more relative mean scatter for ammonia and the most scatter for propylene. SCIPUFF VG data

indicate the least scatter with propylene, followed closely by ethylene, and the most relative mean scatter for the ammonia. The SCIPUFF VG data for ammonia are nearly 25 times greater than the VG data for propylene and ethylene.

The MG data correlation for chemical species shows that ALOHA has the least amount of geometric mean bias for ammonia, followed by slightly more bias with propylene, and even more bias with ethylene. All the MG data for ALOHA indicate an under-prediction bias. The MG data for EPIcode indicate an over-prediction bias for ammonia and ethylene and a small under-prediction bias for propylene. The SCIPUFF MG data indicate the least under-prediction bias for ethylene with slightly more under-prediction bias for propylene and, finally, ammonia.

Table 9 Release Duration Statistical Data

| Factor | Short Flow (5 Min) | | | Long Flow (20+ min) | | |
|---|---|---|---|---|---|---|
| | ALOHA | EPIcode | SCIPUFF | ALOHA | EPIcode | SCIPUFF |
| FAC2 | 0.4231 | 0.3269 | 0.3654 | 0.3824 | 0.5588 | 0.4706 |
| R | -0.0749 | -0.0282 | 0.1878 | 0.1489 | -0.2222 | 0.1327 |
| NMSE | 9.2247 | 3.6747 | 3.1152 | 4.6253 | 2.8258 | 0.9428 |
| FB | 0.8647 | -0.2700 | 0.1834 | 0.8637 | 0.3775 | -0.3697 |
| VG | 216.0872 | 29.5238 | 21.2053 | 26.9466 | 20.4584 | 257.6365 |
| MG | 1.8180 | 0.6392 | 0.5266 | 1.5953 | 0.8020 | 0.3770 |

Table 9 shows the correlation between release duration and model performance. There are 13 short flow data sets and 17 long flow data sets. The FAC2 values are relatively consistent between the two release durations, with ALOHA showing closer agreement for short duration releases, while the EPIcode and SCIPUFF models show closer agreement to the observed data for the long duration releases.

The correlation data indicate a slight increase in correlation between the 5 min and 20 min duration release data sets for all three models. This makes sense considering the fact that the longer duration releases are less likely to produce observations at the extreme. It is much more likely that the short duration releases will miss entire receptor rings, while the longer releases are more likely to be detected across the sensor array.

The NMSE values for all three models show less deviation between predicted and observed data for the short duration releases compared to the long duration releases. SCIPUFF has the lowest NMSE values for both release durations, followed by EPIcode and then ALOHA.

Analysis of the FB data for release duration shows that the ALOHA predictions have slightly less under-prediction bias for the short duration releases compared to the long duration releases. EPIcode FB data show a moderate over-prediction bias with short duration releases and a moderate under-prediction bias with long duration releases. SCIPUFF FB data show a small under-prediction bias for the short duration releases and a moderate over-prediction bias for the long duration releases.

The VG data correlation for release duration indicates ALOHA and EPIcode have less relative mean scatter with the longer duration releases compared to the shorter releases. The ALOHA data are particularly interesting in that the relative mean scatter for the short duration is an order of magnitude higher than for the long duration releases. The SCIPUFF VG data are the opposite of ALOHA, with the long duration data having an order of magnitude greater relative mean scatter than the short duration release data. EPIcode is relatively consistent between the two release durations.

The MG correlation data for release duration indicate less mean geometric bias for the longer duration releases compared to short duration releases for ALOHA and EPIcode, while SCIPUFF MG data indicate slightly less mean geometric bias for short duration releases compared to the long duration releases. EPIcode and SCIPUFF show a geometric mean over-prediction bias for both release durations, while ALOHA shows a geometric mean under-prediction bias for both durations.

# CHAPTER 5

# SUMMARY CONCLUSIONS AND RECOMMENDATIONS

The goal of this study is to determine which model predictions most closely correlate with the observed data and to test the hypothesis that Gaussian dispersion models over-predict plume concentrations in low wind speed conditions. The FAC2 data, as shown in Figure 10, indicate that EPIcode is in closest agreement with the observed data.

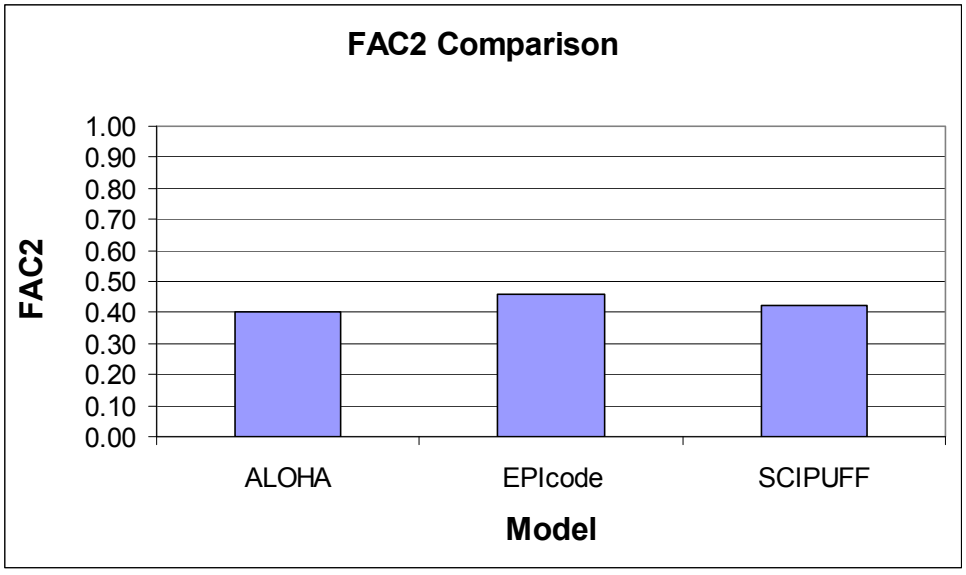


*Figure 10 FAC2 Data versus Model*

Figures 11 and 12 show the over-prediction versus under-prediction bias for the three models.

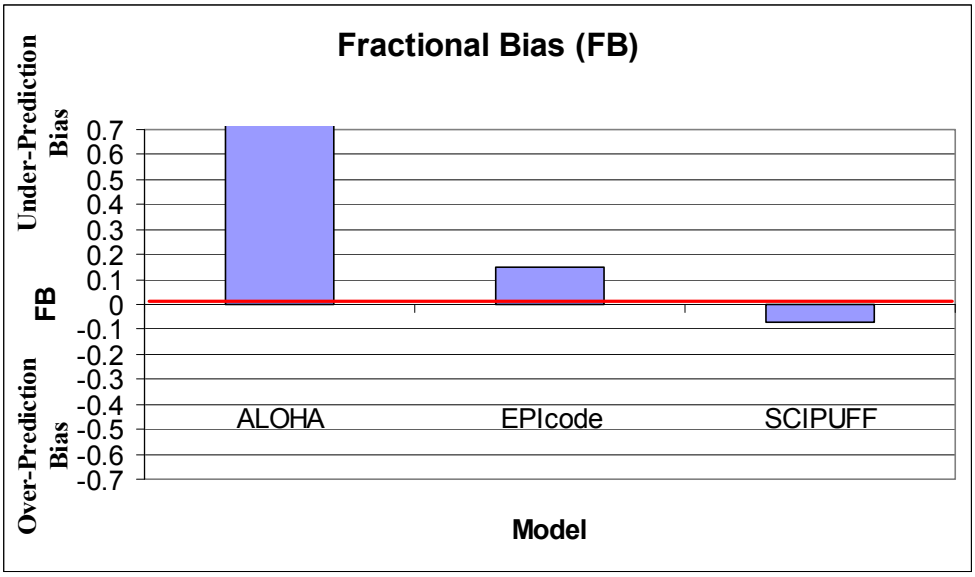


*Figure 11 FB Data versus Model*

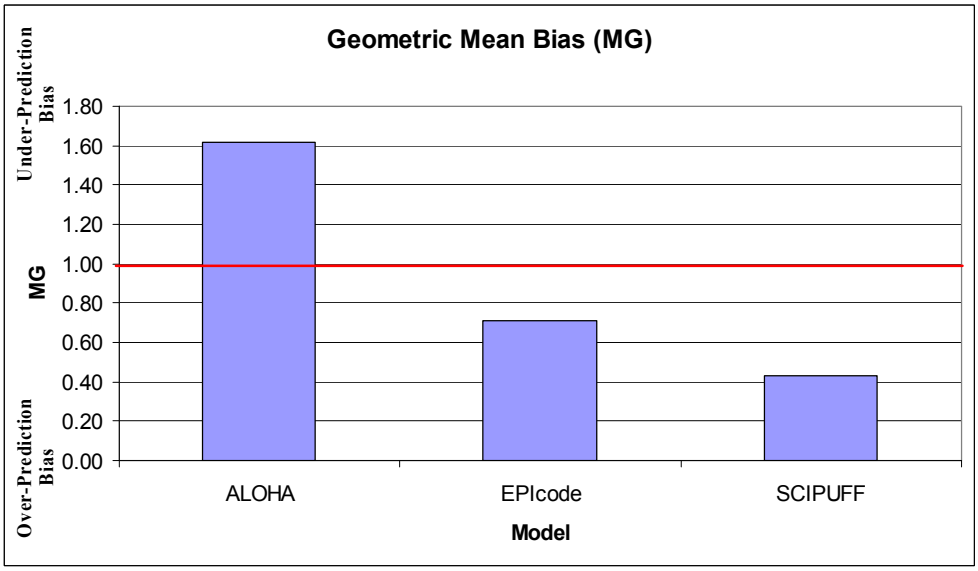


*Figure 12 MG Data versus Model*

The results of these experiments demonstrate that the SCIPUFF model predictions agree with the hypotheses that Gaussian plume dispersion models tend to over-predict downwind plume concentrations in low wind conditions. The EPIcode analysis is not as clear. While the FB data indicate a slight under-prediction bias, the MG data indicate a slight over-prediction bias. Just considering the number of under-predictions versus over-predictions of all the data sets, EPIcode over-predicted the concentrations nearly twice as often as it under-predicted. Since the FB data compare the mean observed and predicted values, the data are weighted for higher values; a few very large value under-predictions can outweigh many small value over-predictions. This suggests that EPIcode over-predicts at low values and under-predicts at high values.

The ALOHA predictions agree with the null hypotheses that models under-predict downwind plume concentration in low wind conditions. The tendency of ALOHA to under-predict can be attributed to the model forcing higher wind speeds than the input data based on internal model parameters that did not allow for the use of the actual observed meteorological data. ALOHA has minimum wind speeds for each stability class. In 19 out of 30 experiments, the observed wind speeds were below the minimum allowable wind speed input for the observed stability class. In each of the 19 cases, ALOHA forced a higher wind speed input, resulting in a lower predicted concentration.

The statistical analysis demonstrated that the EPIcode predictions were the most consistent with observations, with approximately 46% of model predictions within a factor of 2 of the observations. SCIPUFF was next with approximately 42% of predicted values within a factor of 2 of observations, and ALOHA produced nearly 40% of its predictions within a factor of 2 of the observed values. Considering the significant

uncertainty associated with low wind speed plume dispersion, the FAC2 values seem very reasonable.

This experiment was set up to collect data relating to how models perform based on distance from the release point, mass flow rate, molecular weight, and duration of the release. The downwind distance comparison showed the highest correlation between model prediction and observation at the middle rings and significant deviation from observation at the inner-most and outer-most rings for ALOHA and EPIcode, while SCIPUFF predictions were closest to observation for the 10 and 25 m distances, followed by the 100 m and, finally, the 50 m distance. The mass flow rate comparison shows slightly more consistent results from high flow releases compared to low flow releases. However, this data may be somewhat skewed in that the low flow data are predominantly ammonia, while the high flow data do not include any ammonia. Given the models' poor performance in predicting ammonia concentrations, the mass flow rate analysis should not be given too much weight in the overall analysis.

The use of ammonia, ethylene, and propylene was designed to detect any bias in how the models would predict based on molecular weight. ALOHA and EPIcode were most accurate in predicting ethylene concentrations. Ethylene, with a molecular weight nearly that of air, acts as a neutrally buoyant gas. The ammonia, which is lighter than air and acts as a buoyant gas, and the propylene, which is heavier than air and acts as a dense gas, both produced model predictions that were less consistent with observations than the ethylene predictions. In contrast, SCIPUFF was the most accurate with propylene, followed by ammonia then ethylene. The release duration comparison was consistent

with the hypothesis that the longer duration releases will result in less data scatter with less chance of extreme values in the prediction versus observation data sets.

In summary, all three models performed reasonably well considering the significant uncertainty associated with low wind speed releases. However, for purposes of this analysis, EPIcode was the most accurate. EPIcode was also the easiest model to use. It comes with an extensive chemical database, and, since it generally over-predicted, it is considered a conservative model for downwind chemical concentration prediction. This experiment also demonstrated that caution should be exercised when using ALOHA to model low wind speed releases. The model is not designed for such conditions and the predictions tend to under-predict observed concentrations.

The results of this field experiment should be expanded upon, and additional field experiments in low wind speed conditions are recommended. A close examination of the 120 observed data points reveals that 16 of those data points show a higher concentration as the plume traveled downwind. This is due to several factors including plume meander, lofting, and the distance between the point sensors. Increased sensor density will significantly enhance the data product of such research and could greatly expand our ability to validate plume dispersion model predictions in low wind conditions. The additional studies should consider a variety of chemicals to verify the bias of the models towards neutrally buoyant species.

# REFERENCES


Chang, J. and Hanna, S. (2004) *Air quality model performance evaluation*. Meteorology and Atmospheric Physics Vol. 87 (1-3): 167-196.

Cirillo, M. and Poli, A. (1992). *An Intercomparison of Semiempirical Diffusion Models Under Low Wind Speed, Stable Conditions.* Atmospheric Environment Vol. 26A (5): 765-774.

Hanna, S. (1983). *Lateral Turbulence Intensity and Plume Meandering During Stable Conditions*. Journal of Climate and Applied Meteorology Vol. 22: 1,424-1,430.

Hanna, S., Britter, R., and Franzese, P. (2003). *A baseline urban dispersion model evaluated with Salt Lake City and Los Angeles tracer Data*. Atmospheric Environment Vol. 37 (36): 5,069-5,082.

Hanna, S. and Chang, J. (2001). *Use of Kit Fox field data to analyze dense gas dispersion modeling issues*. Atmospheric Environment Vol. 35 (13): 2,231-2,242.

Hanna, S., Chang, J., and Strimaitis, D. (1993). *Hazardous Gas Model Evaluation with Field Observations*. Atmospheric Environment Vol. 27A (15): 2,265-2,285.

Hanna, S. and Chang, J. (1992). *Boundary-Layer Parameterizations for Applied Dispersion modeling over Urban Areas*. Boundary-Layer Meteorology Vol. 58 (3): 229-259.

Hanna, S., Briggs, G., and Hosker, R. (1982). *Handbook on Atmospheric Dispersion, DOE/TIC-11223*. Technical Information Center, U.S. Department of Energy.

Lin, J. and Hildemann, L. (1996). *Analytical Solutions of the Atmospheric Diffusion Equation with Multiple Sources and Height Dependent Wind Speed and Eddy Diffusivities*. Atmospheric Environment Vol. 30 (2): 239-254.

Macdonald, R. (2003). *Theory and Objectives of Air Dispersion Modeling*. MME 474A Wind Engineering. http://www.engga.uwo.ca/people/esavory/MME474A_Part1.pdf

Moreira, D., Tirabassi, T., and Carvalho, J. (2005). *Plume dispersion simulation in low wind conditions in stable and convective boundary layers*. Atmospheric Environment Vol. 39 (20): 3,643-3,650.

Oettl, D., Goulart, A., Degrazia, G., and Anfossi, D. (2005). *A new hypothesis on meandering atmospheric flows in low wind speed conditions*. Atmospheric Environment Vol. 39 (9): 1,739-1,748.

Oreskes, N., Schrader-Frechette, K., and Belitz, K. (1994). *Verification, Validation, and Confirmation of Numerical Models in the Earth Sciences*. Science Vol. 263 (5147): 641-646.

Peterson, H., Mazzolini, D., O'Neill, S., and Lamb, B. (1999). *Instantaneous Spread of Plumes in the Surface Layer*. Journal of Applied Meteorology Vol. 38 (3): 343-352.

Seinfeld, J. and Pandis, S. (1998). *Atmospheric Chemistry and Physics*. John Wiley & Sons, Inc.

Sharan, M., Yadav, A. and Modani, M. (2002). *Simulation of short-range diffusion experiment in low-wind convective conditions*. Atmospheric Environment Vol. 36 (11): 1901-1906.

Sharan, M., Singh, M., and Yadav, A. (1995) *Mathematical Model for Atmospheric Dispersion in Low Winds With Eddy Diffusivities as Linear Functions of Downwind Distance.* Center for Atmospheric Sciences, Indian Institute of Technology, Hauz Khas, New Delhi, India.

Thoman, D., Davis, M., and O'Kula, K. (2005). *A Comparison of EPIcode and ALOHA Calculations for Pool Evaporation and Chemical Atmospheric Transport and Dispersion*. EFCOG Safety Analysis Working Group.

U.S. Department of Energy Office of Environment, Safety and Health, (2004). *EPIcode Computer Code Application Guidance for Documented Safety Analysis*", Office of Quality Assurance Programs.

U.S. Environmental Protection Agency, Technology Transfer Network, FARA (Fate, Exposure, and Risk Analysis), (2004). *Air Toxics Risk Assessment Reference Library*. Vol. 1, Ch. 9. http://www.epa.gov/ttn/fera/risk_atra_vol1.html

Venkatram, A., Isakov, V., Yuan, J., and Pankratz, D. (2004). *Modeling dispersion at distances of meters from urban sources*. Atmospheric Environment 38: 4,633-4,641.

Wang, I. (1996). *Determination of Transport Wind Speed in the Gaussian Plume Diffusion Equation for Low-Lying Point Sources*. Atmospheric Environment Vol. 30 (4): 661-665.

Wieringa, J. (1993). *Representative Roughness Parameters for Homogeneous Terrain.* Boundary Layer Meteorology Vol. 63: 323-363.

Yadav, A. and Sharan, M. (1996). *Statistical Evaluation of Sigma Schemes for Estimating Dispersion in Low Wind Conditions*. Atmospheric Environment Vol. 30 (14): 2,595-2,606.

This manuscript has been authored by National Security Technologies, LLC, under contract No. DE-AC52-06NA25946 with the U.S. Department of Energy. The United States Government retains and the publisher, by accepting the article for publication, acknowledges that the United States Government retains a non-exclusive, paid-up, irrevocable, world-wide license to publish or reproduce the published form of this manuscript, or allow others to do so, for United States Government purposes.